

## ORIGINAL ARTICLE

# Autophagy is required for cell survival under L-asparaginase-induced metabolic stress in acute lymphoblastic leukemia cells

H Takahashi<sup>1,2,3</sup>, J Inoue<sup>1,3</sup>, K Sakaguchi<sup>2</sup>, M Takagi<sup>4</sup>, S Mizutani<sup>4</sup> and J Inazawa<sup>1,3</sup>

L-asparaginase has been used for more than three decades in acute lymphoblastic leukemia (ALL) patients and remains an essential drug in the treatment of ALL. Poor response to L-asparaginase is associated with increased risk of therapeutic failure in ALL. However, both the metabolic perturbation and molecular context of L-asparaginase-treated ALL cells has not been fully elucidated. Here we identify that treatment with L-asparaginase results in metabolic shutdown via the reduction of both glycolysis and oxidative phosphorylation, accompanied by mitochondrial damage and activation of autophagy. The autophagy is involved in reducing reactive oxygen species (ROS) level by eliminating injured mitochondria. Inhibition of autophagy enhances L-asparaginase-induced cytotoxicity and overcomes the acquired resistance to L-asparaginase in ALL cells. The ROS-p53-positive feedback loop is an essential mechanism of this synergistic cytotoxicity. Thus, our findings provide the rationale for the future development of combined treatment of L-asparaginase and anti-autophagy drug in ALL patients.

*Oncogene* (2017) 36, 4267–4276; doi:10.1038/onc.2017.59; published online 27 March 2017

## INTRODUCTION

Acute lymphoblastic leukemia (ALL) is the most common type of childhood cancer.<sup>1</sup> Although treatment outcomes have been remarkably improved by the development of effective therapies and well-designed protocols, ~20% of pediatric patients develop resistance to therapy and eventually relapse, often leading to death.<sup>1,2</sup> L-asparaginase (L-asp), one of the most important drugs used for childhood ALL therapy, is an enzyme that catalyzes the hydrolysis of asparagine (Asn) or glutamine (Gln) to aspartic acid or glutamic acid, respectively.<sup>3</sup> Poor response to L-asp is associated with increased risk of relapse and therapeutic failure.<sup>4,5</sup> It has been proposed that the sensitivity of ALL to L-asp is due to low or absent expression of asparagine synthetase.<sup>6–8</sup> However, genome-wide expression profiling of ALL patient samples showed conflicting results,<sup>9–11</sup> and basal asparagine synthetase expression was shown to have no clinical significance in ALL patients.<sup>12</sup> Thus, despite long-standing experience with L-asp therapy, both the metabolic perturbation and molecular context of L-asp-treated ALL cells remains to be fully elucidated.

One of the major cellular responses to amino-acid depletion is the induction of autophagy. Autophagy is a degradation process of proteins and organelles, which can provide metabolic intermediates such as amino acids, and can also reduce reactive oxygen species (ROS)-mediated oxidative stress by eliminating damaged mitochondria.<sup>13</sup> Some anticancer drugs can induce cytoprotective autophagy,<sup>14</sup> and several clinical trials using combined treatment of existing anticancer drugs and the lysosomal inhibitor chloroquine (CQ) are currently ongoing.<sup>15</sup> Treatment with L-asp can also induce cytoprotective autophagy in

human cancers.<sup>16–18</sup> However, the biological significance of L-asp-induced autophagy or the effect of autophagy inhibition in L-asp-treated cells remains largely unknown. In this study, we sought to reveal how L-asp affects cellular processes in ALL cells, and to elucidate the implication of L-asp-induced autophagy in hopes of obtaining insight into alternative strategies for ALL therapy.

## RESULTS

L-asp treatment induces metabolic shutdown and mitochondrial injury in ALL cells

We first confirmed that intracellular Asn and Gln were immediately depleted in REH cells during L-asp treatment (Figure 1a). To understand the physiological effect of L-asp treatment, we next performed the gene expression array of L-asp-treated REH cells, accompanied by gene ontology (GO) analysis using Database for Annotation, Visualization, and Integrated Discovery (DAVID)<sup>19</sup> and gene set enrichment analysis.<sup>20</sup> The expression levels of genes associated with several cellular metabolic pathways, including glycolysis, tricarboxylic acid cycle and oxidative phosphorylation, were significantly lower in L-asp-treated REH cells than in untreated cells (Figures 1b and c and Supplementary Table S2). Decreased expression levels of these metabolism-related genes were also confirmed in two ALL cell lines, REH and 697, by qRT-PCR (Figure 1d and Supplementary Figure S1). These findings were consistent with the decrease of intracellular ATP level (Figure 1a) and the result from the energy metabolism analysis using the XF24 extracellular flux analyzer; basal levels of both the oxygen consumption rate (OCR) for oxidative phosphorylation in the mitochondria and the extracellular acidification rate

<sup>1</sup>Department of Molecular Cytogenetics, Medical Research Institute, Tokyo Medical and Dental University (TMDU), Tokyo, Japan; <sup>2</sup>Department of Pediatrics, Hamamatsu University School of Medicine, Shizuoka, Japan; <sup>3</sup>Bioresource Research Center, Tokyo Medical and Dental University (TMDU), Tokyo, Japan and <sup>4</sup>Department of Pediatrics and Developmental Biology, Tokyo Medical and Dental University (TMDU), Tokyo, Japan. Correspondence: Dr J Inoue or Professor J Inazawa, Department of Molecular Cytogenetics, Medical Research Institute, Tokyo Medical and Dental University (TMDU), 1-5-45 Yushima, Bunkyo-ku, Tokyo 113-8510, Japan. E-mail: jun.cgen@mri.tmd.ac.jp or johinaz.cgen@mri.tmd.ac.jp

Received 20 September 2016; revised 31 January 2017; accepted 7 February 2017; published online 27 March 2017

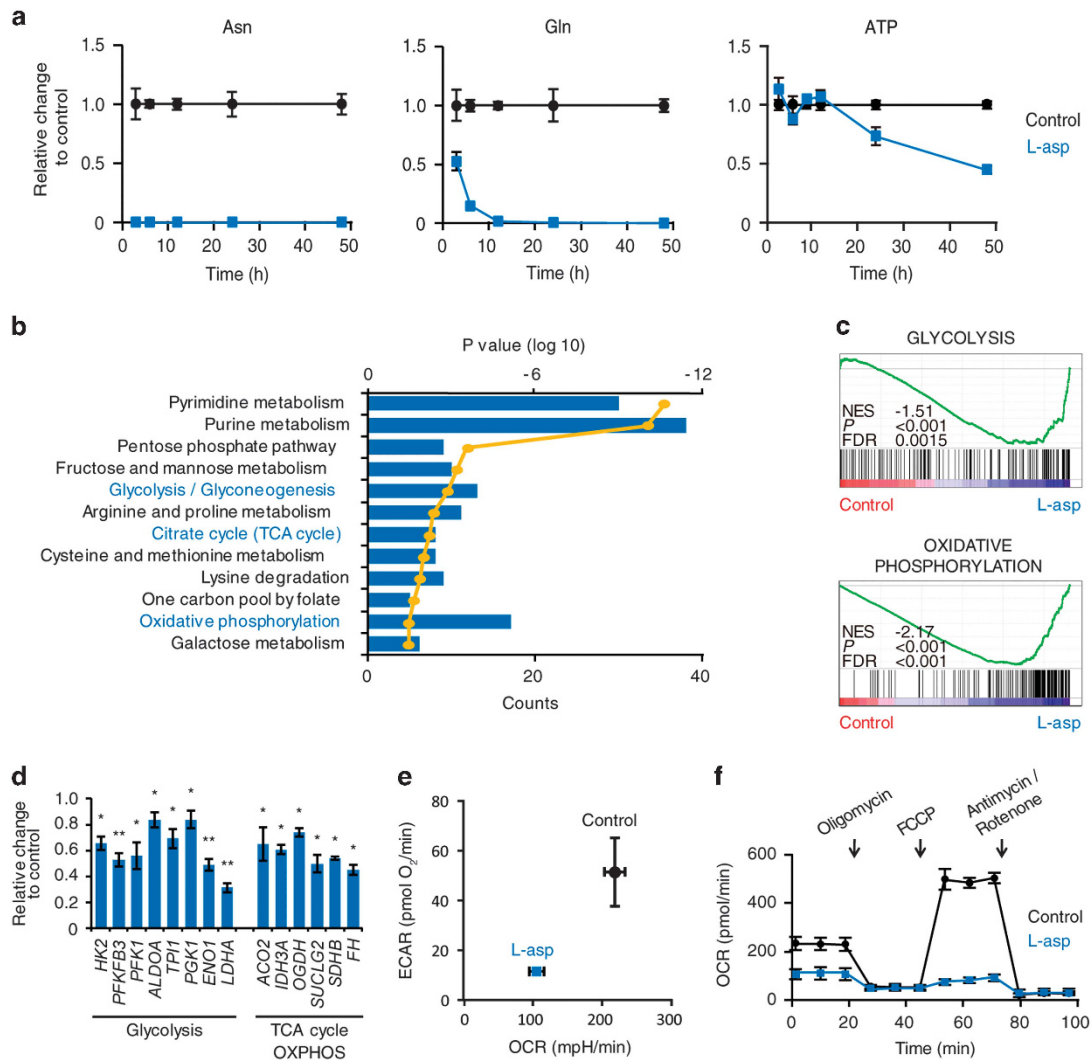


**Figure 1.** Induction of metabolic shutdown by L-asparaginase treatment. **(a)** Intracellular analysis of asparagine, glutamine and ATP. REH cells were treated with 1 U/ml of L-asp for the indicated time. Data are represented as relative ratio to control at each incubation time. **(b)** Expression array analysis in L-asp-treated REH cells. REH cells were treated with 1 U/ml of L-asp for 48 h. GO terms associated with metabolism from DAVID analysis. All candidate GO terms are ranked by *P*-value, and are listed in Supplementary Table S2. Bars indicate the counts of genes included in the respective gene set for each GO term. Line indicates *P*-values in log<sub>10</sub>. **(c)** Gene set enrichment analysis (GSEA) of microarray expression data comparing untreated and L-asp-treated REH cells. NES, normal enrichment score. **(d)** Quantitative RT-PCR analysis for glycolysis-, tricarboxylic acid (TCA) cycle- and OXPPOS-related genes in L-asp-treated REH cells (1 U/ml of L-asp for 48 h). Expression of  $\beta$ -actin was used as an internal control. Expression levels relative to those in the untreated cells are indicated on the vertical axis. *P*-values were calculated using two-sided Student's *t*-test (\**P* < 0.05, \*\**P* < 0.01). **(e)** Absolute OCR and ECAR values of untreated and L-asp-treated REH cells (1 U/ml of L-asp for 48 h). **(f)** Mitochondria stress test in untreated and L-asp-treated cells. OCR levels were calculated by normalization to cell number.

(ECAR) for glycolysis were remarkably lower in L-asp-treated cells than in untreated cells (Figure 1e), suggesting that L-asp treatment effectively induces metabolic shutdown in ALL cells. In a mitochondrial stress test, treatment with oligomycin, an Fo-ATPase inhibitor of Complex V, clearly reduced mitochondrial respiration in L-asp-treated and untreated cells. However, spare respiratory capacity (defined as the quantitative difference between maximal OCR after addition of mitochondrial oxidative phosphorylation uncoupler carbonyl cyanide 4-(trifluoromethoxy) phenylhydrazone and the initial basal OCR) in L-asp-treated cells was significantly lower than in untreated cells (Figure 1f). These data suggested that L-asp treatment induces metabolic shutdown accompanied by reduction of both glycolysis and oxidative phosphorylation, and mitochondrial function is heavily impaired in L-asp-treated cells.

L-asp-induced autophagy is involved in reducing ROS level by eliminating injured mitochondria

To investigate whether L-asp treatment induced autophagy in ALL cells, we next evaluated autophagy flux in ALL cells by detection of LC3B form-II (LC3B-II), an autophagosome marker.<sup>21</sup> By western blotting, LC3B-II levels were observed to be increased by L-asp treatment, and this increase was significantly enhanced by inhibiting autophagosome turnover via the addition of a lysosomal inhibitor, CQ or bafilomycin A1 (Baf; Figure 2a and Supplementary Figure S2A). In immunofluorescence analysis, LC3B-positive autophagic puncta were observed in L-asp-treated REH cells, and the number of these puncta was remarkably increased by the addition of CQ (Figure 2b). Moreover, electron microscopic analysis revealed that both the number and area of autophagic vacuoles per cell were significantly increased in

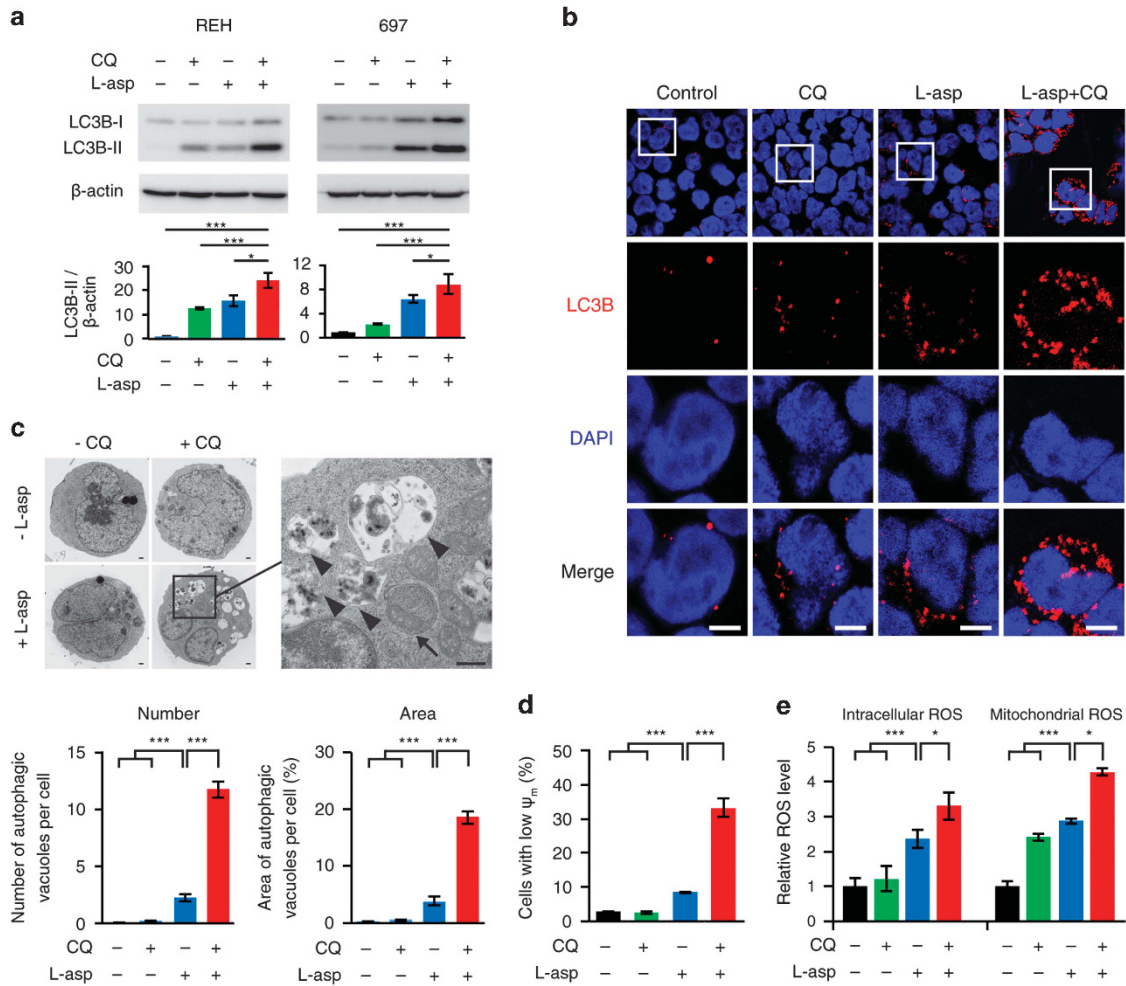


**Figure 2.** Induction of autophagy by L-asparaginase treatment. **(a)** Western blot analysis of REH and 697 cells. Fold change of LC3B-II level (normalized to  $\beta$ -actin) relative to that of untreated cells is indicated in the graph in the lower panel. **(b)** Immunofluorescence analysis of LC3B protein. Square areas are enlarged and shown in the lower panel. Scale bars represent 10  $\mu$ m. **(c)** Representative images of electron microscopic analysis. Arrow and arrowhead indicate an autolysosome and autophagosome, respectively. Numbers and areas of these autophagic vacuoles per cell were analyzed using ImageJ. Fifty cells were investigated per group. Scale bars represent 500 nm. Data represent as mean  $\pm$  s.d. **(d)** Mitochondrial membrane potential assay with TMRE. Fluorescence intensity was measured using flow cytometry. **(e)** Measurement of intracellular and mitochondrial ROS level. Treated REH cells were stained with 10  $\mu$ M of DCFDA (intracellular ROS) or 2.5  $\mu$ M of MitoSox (mitochondrial ROS). REH cells were treated with 1 U/ml of L-asp for 48 h and/or 10  $\mu$ M of CQ for the last 3 h (**a–d**) or for 48 h (**d, e**). Data in **a, c–e** represent as mean  $\pm$  s.d. ( $n=3$ ); \* $P < 0.05$ , \*\*\* $P < 0.001$ .  $P$ -values were calculated using one-way analysis of variance (ANOVA).

L-asp-treated REH cells, and these increases were clearly enhanced by addition of CQ (Figure 2c). These findings suggest that L-asp treatment can induce autophagy in ALL cells.

Furthermore, intracellular amino-acid profiles revealed that both Asn and Gln levels rapidly decreased after L-asp treatment; however, the rate of decrease of these amino acids in the L-asp-treated cells did not significantly differ between cells treated with or without CQ (Supplementary Figure S2B), suggesting that autophagy might not contribute to supply a detectable amount of these amino acids. In contrast, the feature of mitochondrial injury such as the decreased mitochondrial membrane potential ( $\psi_m$ ) and the increase in both intracellular and mitochondrial ROS levels were remarkably enhanced autophagy-inhibited REH cells during L-asp treatment (Figures 2d and e and Supplementary Figures S2C–E). In addition, L-asp treatment significantly induced a decrease in the amount of mitochondrial DNA and mitochondrial mass (Supplementary Figures S2F and G). Taken together, these data suggested that L-asp-induced autophagy functions predominantly in mitochondrial quality control rather than in recycling intracellular amino acids. Autophagy inhibition enhances the

cytotoxicity of L-asparaginase treatment. We then examined the effect of autophagy inhibition on L-asp-induced cytotoxicity in ALL cell lines. When autophagic degradation was pharmacologically inhibited by treatment with CQ simultaneously with L-asp treatment, the number of dead cells remarkably increased compared to L-asp alone (Figure 3a). Apoptotic cells, indicated by increased levels of cleaved caspase-3 and cleaved PARP, were clearly detected with combined treatment of L-asp and CQ (Figure 3b). For cell cycle analysis, the treatment with L-asp alone induced cell cycle arrest at the G1 phase, consistent with a previous report,<sup>22</sup> and the combined treatment with CQ and L-asp significantly increased the sub-G1 population (Supplementary Figure S3A). Concurrent treatment with the caspase inhibitor zVAD-fmk inhibited the induction of cell death by combined treatment of L-asp and CQ (Supplementary Figure S3B). Treatment of ALL cells with L-asp showed significantly synergistic antileukemic effects in combination with autophagy inhibition using CQ (combination index at the IC50=0.515 in REH cells and 0.686 in 697 cells; Supplementary Figure S3C). We next investigated the effect of prolonged treatment exposure with L-asp. Almost all cells



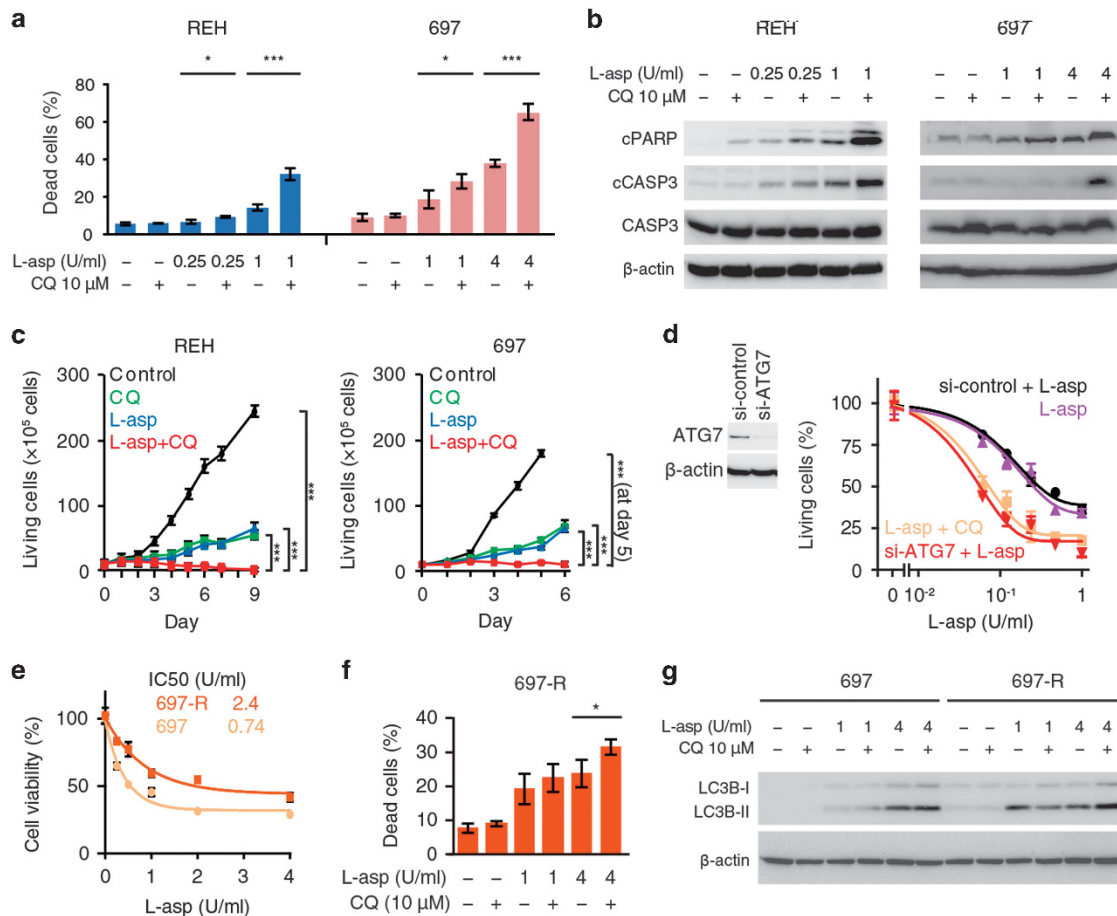


**Figure 3.** Effect of autophagy inhibition on L-asparaginase-induced cytotoxicity in ALL cells. **(a, b)** Apoptotic analysis in ALL cell lines REH and 697 cells with or without CQ treatment by flow cytometry **(a)** and western blotting **(b)**. The proportion of dead cells was measured by flow cytometry using Annexin-V staining. Cells were treated with the indicated concentrations of L-asp and/or CQ for 48 h. **(c)** Cell survival assay during prolonged treatment. According to the clinical method for administering L-asp, which is repeated every 3 days in patients, ALL cells were cultured with PBS (control) or repeated (0, 72, 144 h) administration of L-asp and/or CQ. Viable cells were counted using trypan blue staining every 24 h. ALL cells were treated with repeated administration of L-asp and/or CQ. **(d)** Sensitivity to L-asp treatment in REH cells transfected with ATG7-siRNA. Cells transfected with control-siRNA (si-control) or ATG7-siRNA (si-ATG7) were treated with the indicated concentrations of L-asp for 48 h. Viable cells were counted by flow cytometry using Annexin-V staining. **(e)** Cell survival assay of parental cells and L-asp-resistant cells generated from 697 cells (697-R). **(f)** Apoptotic analysis of 697-R cells. **(g)** Western blot analysis of parental cells and 697-R cells. Data in **a** and **d–f** are represented as mean  $\pm$  s.d. ( $n = 3$ ; \* $P < 0.05$ , \*\*\* $P < 0.001$ ).  $P$ -values were calculated using two-sided Student's  $t$ -test **(a, f)**, and one-way ANOVA **(c)**.

treated with the combination of L-asp and CQ died after 6–9 days, whereas cells treated with L-asp or CQ alone remained viable and continued to slowly proliferate during treatment (Figure 3c). This combined effect was also observed when autophagy was inhibited by small interference RNA (siRNA)-mediated knockdown of the essential autophagy genes including *ATG7*, *ATG5* and *BECLIN1* (*Beclin1*; Figure 3d and Supplementary Figure S3D). Furthermore, we examined the inhibitory effect of autophagy process at the early stage by treatment with 3MA or at the late stage by treatment with ALLN, a cathepsin inhibitor. As the result, the clear synergistic effect was shown in both combined treatment, suggesting that blocking autophagy flux can enhance L-asp-induced toxicity in ALL cells (Supplementary Figures S3E and F). Particularly, the synergistic effect by CQ treatment was not shown in the cells whose autophagy was clearly inhibited by treatment with 3MA (Supplementary Figure S3G), suggesting that CQ-mediated sensitization is dependent on inhibiting autophagy. To test whether autophagy inhibition can overcome the resistance to L-asp treatment, we generated the acquired resistant cells from 697 cells by prolonged exposure to L-asp (parental 697 cells; IC50=0.74 and 697-R cells, a resistant 697 cell; IC50=2.4;

Figure 3e). Combined treatment of L-asp and CQ induced significant cell death, including in 697-R cells (Figure 3f). Importantly, LC3B-II levels were increased in 697-R cells more than in parental 697 cells by L-asp treatment, and this increase was significantly enhanced by CQ treatment, suggesting that the activity of L-asp-induced autophagy in 697-R cells was higher than that of the parental 697 cells (Figure 3g). Thus, these findings suggest that autophagy inhibition may be a useful strategy to overcome L-asp resistance. Combination treatment of L-asp and chloroquine suppresses leukemia growth *in vivo*. To examine the therapeutic potential of the combined treatment using an *in vivo* ALL xenograft model, REH cells stably expressing luciferase (REH-Luc2) were injected into the tail vein of non-obese diabetic/severe combined immunodeficient mice. Quantification of leukemia-associated bioluminescence at 7 days after transplantation demonstrated no significant differences among the four treatment groups (Figure 4a). The mice then received daily intraperitoneal injections of PBS, 6 U/g L-asp, 50 mg/kg CQ or both L-asp and CQ. Asn levels in the plasma of mice treated with L-asp were completely depleted (Figure 4b). A decrease in leukemia burden and increase in outcome improvement were observed in mice

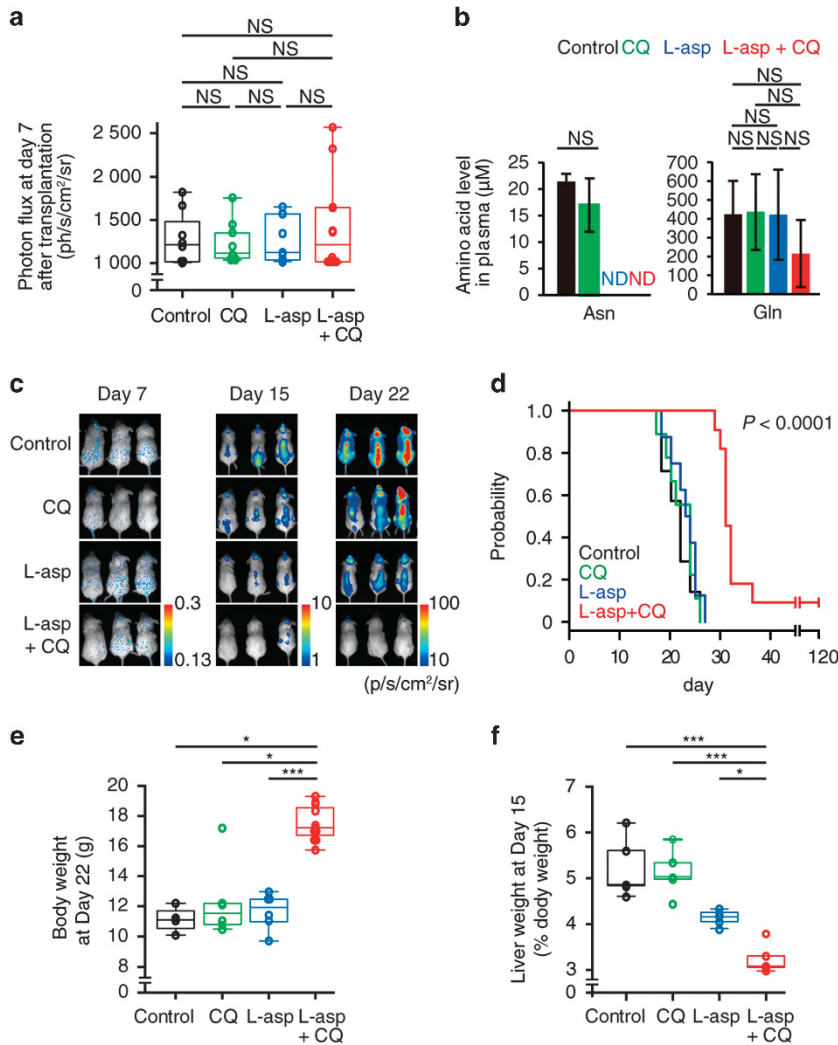


**Figure 4.** Therapeutic potential of autophagy inhibition upon treatment with L-asparaginase in ALL xenograft model. **(a)** Quantification of bioluminescent signals in mice transplanted with luciferase-transduced REH cells on day 7 after transplantation. The graph indicates that no significant difference was observed among the four treatment groups (control,  $n = 7$ ; CQ,  $n = 9$ ; L-asp,  $n = 8$ ; L-asp+CQ,  $n = 11$ ) in photon flux. **(b)** Measurement of peripheral amino-acid levels by LC-MS/MS. Samples were prepared from the plasma of mice on day 14 after administration in independent experiments. The levels were normalized to the volume of drawn blood. Data represent as mean  $\pm$  s.d. ( $n = 3$ ). **(c)** Whole-body mouse imaging. A pseudocolor scale shows relative bioluminescence changes over time. **(d)** Kaplan–Meier overall survival curve in mice treated with PBS only (control,  $n = 7$ ), CQ (50 mg/kg,  $n = 9$ ), L-asp (6 U/g,  $n = 8$ ) or L-asp plus CQ (6 U/g and 50 mg/kg, respectively,  $n = 11$ ). **(e)** Body weight on day 22 after transplantation (control,  $n = 7$ ; CQ,  $n = 9$ ; L-asp,  $n = 8$ ; L-asp+CQ,  $n = 11$ ). **(f)** Liver weight (% body weight) of control or treated mice. Mice were killed on day 15 after transplantation ( $n = 5$  per group).  $P$ -values were calculated using one-way ANOVA (**a**, **b**, **e**, **f**) and log-rank test (**d**); \* $P < 0.05$ , \*\*\* $P < 0.001$ ; ND, not detected; NS, not significant).

administered L-asp and CQ combined treatment, compared with mice treated with L-asp or CQ alone (Figures 4c and d and Supplementary Figure S4A). This therapeutic effect by combined treatment with L-asp and CQ was also observed in other xenograft models using 697-Luc2 cells (Supplementary Figures S4B and C). As hepatomegaly is caused by infiltration of leukemia cells, the liver weight of mice with leukemia is used as the indicator of objective response to antileukemic agents on some occasions.<sup>23,24</sup> Mice treated with L-asp or CQ alone were found to have significantly decreased body weight and increased liver weight compared with mice administered L-asp and CQ combined treatment (Figures 4e and f), which indicate a remarkable antileukemic response. In addition, we could not find any signs of the treatment-related complication including hemorrhage or infarction in the killed mice. Importantly, LC3B-positive puncta were observed to be accumulated in ALL cells that remained within the bone marrow, peripheral blood and central nervous

system of the mice receiving combined treatment, indicating the therapeutically sufficient autophagy inhibition (Supplementary Figure S5). These findings strongly suggested that combined treatment with L-asp and CQ may be therapeutically useful for ALL.

The ROS-p53-positive feedback loop is an essential mechanism of the combined treatment of L-asp and CQ

We attempt to determine the molecular mechanism underlying the synergistic effect of L-asp-induced cytotoxicity and autophagy inhibition. Although the apoptosis pathway via the ATF4-CHOP axis is known to be involved in L-asp-induced cytotoxicity,<sup>25</sup> this pathway was not significantly activated in cells treated with the combination of L-asp and CQ, compared with the cells treated with L-asp alone (Supplementary Figure S6), suggesting that other mechanisms may contribute to the induction of cell death by

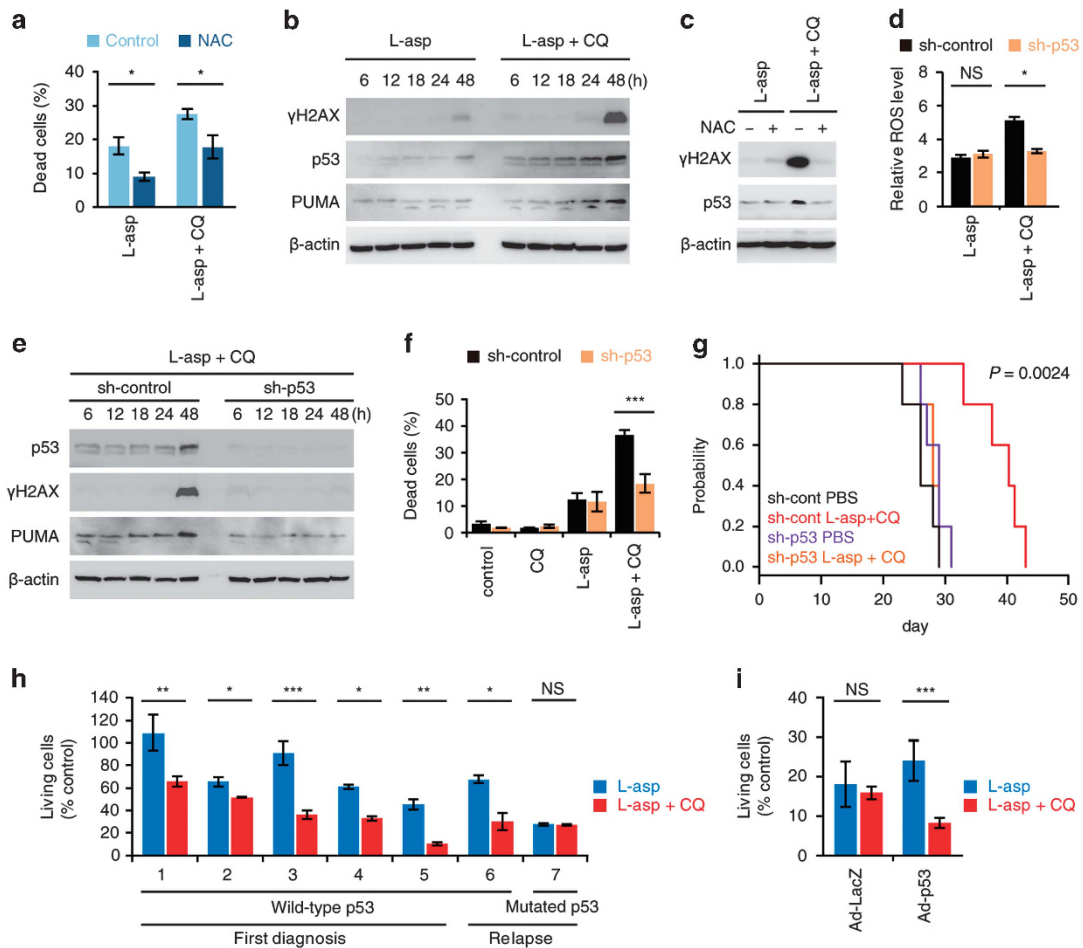


**Figure 5.** Activation of the ROS-p53 feedback loop by combination treatment of L-asparaginase and chloroquine in ALL cells. **(a)** Effect of N-acetyl-L-cysteine (NAC) on induction of cell death. REH cells were concurrently treated with 2 mM of NAC with 1 U/ml of L-asp and/or 10  $\mu$ M of CQ for 48 h. **(b)** Western blot analysis of L-asp and/or CQ-treated REH cells. **(c)** Western blot analysis of NAC-treated REH cells. L-asp and/or CQ-treated cells were concurrently treated with 2 mM NAC for 48 h. **(d–f)** Cellular ROS detection assay **(d)**. Western blot analysis **(e)** and apoptosis analysis **(f)** of *TP53*-knockdown REH cells. **(g)** Kaplan–Meier overall survival curve in mice. Non-obese diabetic/severe combined immunodeficient (NOD/SCID) mice were transplanted with REH-Luc2 cells stably transfected with sh-control or sh-p53 by tail vein injection. These mice were treated as described in Figure 4d ( $n = 5$  per group). **(f)** Cell survival assay in primary ALL samples. ALL cells were purified from the bone marrow of samples from ALL patients shown in Supplementary Table S3. Cells were treated with 1 U/ml of L-asp and/or 10  $\mu$ M of CQ for 48 h, and viable cells were measured by flow cytometry using Annexin-V staining. **(g)** Effect of p53 expression on cell survival in ALL cells purified from patient No.7. Cells transfected with Ad-LacZ (as a control) or Ad-p53 were treated with 1 U/ml of L-asp and/or 10  $\mu$ M of CQ for 48 h. Viable cells were measured as described in **h**. Data in **a**, **d**, **f**, **h**, **i** represent as mean  $\pm$  s.d. ( $n = 3$ ); \* $P < 0.05$ , \*\* $P < 0.01$ , \*\*\* $P < 0.001$ ; NS, not significant.  $P$ -values were calculated using two-sided Student's  $t$ -test (**a**, **d**, **f**, **h**, **i**) and log-rank test (**g**).

combined treatment with L-asp and CQ. We then focused on the production of ROS as a possible mechanism because ROS levels were remarkably increased during combined treatment (Figure 2e). ROS scavenger N-acetyl-L-cysteine rescued the induction of cell death by combined treatment with L-asp and CQ (Figure 5a and Supplementary Figure S7A), indicating that excessive ROS accumulation is critical for the induction of cytotoxicity by the combined treatment. Severe ROS accumulation leads to irreparable DNA damage, which may induce the ROS–DNA damage–p53-positive feedback loop.<sup>26</sup> The protein expression levels of p53 and PUMA were remarkably increased, and was accompanied by DNA damage indicated by an increased level of  $\gamma$ H2AX, in cells treated with the combination of L-asp and CQ compared with cells treated with L-asp alone in both REH and 697 cells with *TP53* wild type (Figure 5b and Supplementary Figure S7B). The inhibition of ROS production by treatment with N-acetyl-L-cysteine led to the reduction of both DNA damage and p53 expression (Figure 5c and Supplementary Figure S7C). *TP53* knockdown resulted in the reduction of ROS and DNA damage in

cells treated with the combination of L-asp and CQ (Figures 5d and e and Supplementary Figures S7D and E). *TP53* is known to have multiple roles in the regulation of autophagy.<sup>27</sup> In western blot analysis, knockdown of *TP53* did not exert a severe influence on L-asp-induced autophagy (Supplementary Figures S7F). Importantly, when *TP53* expression was inhibited by differentiating two knockdown systems using short hairpin RNA (shRNA) or siRNA, the synergistic cytotoxic effect of L-asp and CQ combined treatment was abrogated (Figure 5f and Supplementary Figures S7G and H). Activated p53 transcriptionally upregulated the pro-oxidant genes, including *PUMA*, *TP53I3*, *SCO2*, and downregulated the anti-oxidant gene *HK2* (Supplementary Figure S7I). In addition, in overall survival analysis of mice transplanted with *TP53*-knockdown or control ALL cells treated with L-asp and CQ combination, poor outcome was observed in mice transplanted with *TP53*-knockdown ALL cells (sh-p53), similar to those receiving no treatment (Figure 5g). We finally examined the functional role of p53 on the synergistic effect of L-asp and CQ combination treatment in seven primary ALL samples, including six cases with

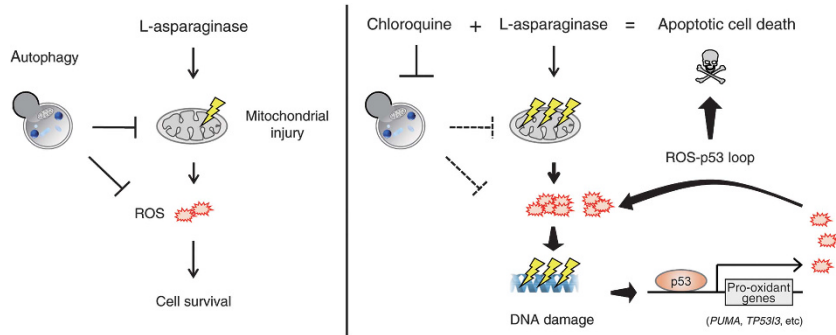


**Figure 6.** Schematic diagram. L-asparaginase treatment induces mitochondrial injury. Autophagy contributes to the prevention of oxidative DNA damage accumulation in L-asparaginase-treated cells. Autophagy inhibition with L-asparaginase treatment triggers the ROS–DNA damage–p53 feedback loop, which leads to marked apoptosis in ALL cells.

wild-type *TP53* and one case with mutant *TP53* (R248Q). These samples were derived from five newly diagnosed patients and two relapsed patients. Clinical features of these patients are shown in Supplementary Table S3. As expected, the synergistic effect of L-asparaginase and CQ was observed in ALL cells derived from the six wild-type *TP53* samples, but not in ALL cells from the mutant *TP53* sample (Figure 5h). In addition, adenovirus-mediated expression of exogenous *TP53* into *TP53*-mutated ALL cells from No.7 patient or *TP53*-mutated ALL cell lines, Jurkat and CCRF-CEM, induced the synergistic effect by combined treatment with L-asparaginase and CQ (Figure 5i and Supplementary Figure S7J). These findings strongly suggest that p53 function is essential for this synergistic effect.

## DISCUSSION

In the present study, we clarified the physiological effect of L-asparaginase and the biological significance of L-asparaginase-induced autophagy, and additionally demonstrated the therapeutic effectiveness of autophagy inhibition by CQ in combination with L-asparaginase treatment in ALL cells. The treatment with L-asparaginase results in metabolic shutdown via the reduction of both glycolysis and oxidative phosphorylation, accompanied by mitochondrial injury and ROS production. Importantly, we demonstrated that the inhibition of autophagy using CQ enhances L-asparaginase-induced cytotoxicity and overcomes the acquired resistance to L-asparaginase in ALL cells via ROS–p53-positive feedback loop as an essential mechanism of this synergistic cytotoxicity (Figure 6).

Several studies have suggested that autophagy may act as a cytoprotective mechanism in tumor cells and that therapy-induced cell death can be enhanced upon autophagy inhibition.<sup>18,28–30</sup> It has been reported that cytoprotective autophagy was induced by treatment with L-asparaginase and autophagy inhibition enhanced L-asparaginase-induced cytotoxicity in K562 cells, a chronic myeloblastic leukemia cell line. However, the functional role of L-asparaginase-induced autophagy has not been clarified. While it has been believed that L-asparaginase-induced autophagy contributes to the supply of amino acids including Asn and Gln,<sup>16–18,31</sup> our data in the current study suggest that L-asparaginase-induced autophagy predominantly have a function as elimination of damaged mitochondria rather than supply of intracellular amino acids by recycling. In treatment of patients with ALL, L-asparaginase is used in combination with vincristine and prednisone.<sup>2</sup> Prednisone is reported to induce autophagy, which is required for cell death.<sup>32–34</sup> Thus, the modulation of autophagy by CQ needs to consider autophagic effect on combined drugs other than L-asparaginase in the clinical setting of ALL.

We demonstrated in an ALL xenograft model that autophagy inhibition using CQ with L-asparaginase treatment is therapeutically effective. Notably, the effect of L-asparaginase and CQ combined treatment could be observed in ALL cells that remained within the bone

marrow and central nervous system, suggesting the potency of autophagy inhibition with CQ in combination with L-asparaginase treatment in intractable ALLs. In addition to clinical trials utilizing the inhibition of autophagy by CQ for treatment of solid tumors in adults, CQ is clinically used as an FDA-approved drug for treatment of pediatric patients with several diseases, such as malaria and interstitial lung disease.<sup>35,36</sup> However, CQ may cause severe side effects, including irreversible retinal toxicity.<sup>36</sup> Moreover, CQ is not a specific autophagy inhibitor, but also modulates various additional signal transduction pathways.<sup>37</sup> Therefore, development of therapeutic agents that can specifically inhibit the autophagy pathway is required for the clinical use.

We showed that functional p53 is needed for the synergistically cytotoxic effect of L-asparaginase and CQ combined treatment in ALL cells. While autophagy was shown to be required for the development of Ras-driven pancreatic tumors in a previous study, autophagy inhibition by CQ promoted tumorigenesis in developing tumors lacking p53.<sup>38</sup> Another study reported that p53 has an important role in the combined effect of temozolomide and CQ in glioblastoma.<sup>39</sup> Thus, these previous reports together with the present results suggest that functional p53 has an essential role in autophagy inhibition-mediated cytotoxicity. Because mutations of the *TP53* gene are observed in ~6–8% of pediatric ALL patients,<sup>40</sup> the majority of pediatric patients may benefit from the combined effect of autophagy inhibition and L-asparaginase treatment.

In summary, we reported molecular evidence supporting the development of a novel therapeutic strategy of combined L-asparaginase and autophagy inhibition for ALL. It will be important for ALL patients to evaluate the autophagy flux before, after or during L-asparaginase treatment. Further validation of this strategy, together with determination of p53 status, in a large cohort of patients is warranted to effectively evaluate its impact on the treatment of ALL.

## MATERIALS AND METHODS

### Cell culture and reagents

*TP53*-intact ALL cell lines, REH and 697, or *TP53*-mutated ALL cell lines, CCRF-CEM and Jurkat, were maintained in RPMI1640 medium supplemented with 10% fetal bovine serum, penicillin and streptomycin. Culture medium was changed 24 h before treatment for each experiment. REH (CRL-8286), CCRF-CEM (CRL-8436) and Jurkat (TIB-152) are commercially available from the American Type Culture Collection, and 697 is available from DSMZ (Germany, catalog code ACC 42). LEUNASE was used for L-asparaginase treatment, purchased from Kyowa Hakko Kirin Co. (Tokyo, Japan). Chloroquine diphosphate, Bafilomycin A1 and N-acetyl-L-cysteine were purchased from Sigma-Aldrich Co. (St. Louis, MO, USA).

### Patients

Bone marrow with more than 90% blast content was obtained from six patients (five patients with newly diagnosed ALL and one patient with



relapsed ALL). Cells were isolated by Ficoll density-gradient separation. Written informed consent was obtained from all of the patients. The collection and analysis of patient samples were approved by the ethics committees of the Tokyo Medical and Dental University Institutional Review Board (approval #2010-5-2) and Hamamatsu University School of Medicine (approval #24-284).

#### Animals

Female non-obese diabetic/severe combined immunodeficient mice were purchased from Charles River Laboratories Japan. ALL cells ( $5 \times 10^6$  per 100  $\mu$ l) infected with a lentiviral vector for *Luc2* were injected into the tail vein of non-obese diabetic/severe combined immunodeficient mice (age 6–8 weeks). Concentration of L-asp dose in *in vivo* experiment was decided using the interview form of LEUNASE as reference. The intraperitoneal lethal dose 50 of LEUNASE in mice was estimated to be 10 U/g; therefore, we performed preliminary experiments and ascertained that our mice had a tolerance to repeated intraperitoneal injection of 6 U/g L-asp and 50 mg/kg CQ administration once every day for more than 50 days. Leukemia burden was measured by luciferase activity using a luminometer (Photon Imager, Biospace Lab, Nesles la Vallée, France) after 150 mg/kg D-luciferin (Synchem UG & Co. KG, Felsberg, Germany) injection. All experimental protocols conducted on the mice were approved by the Tokyo Medical and Dental University Animal Care and Use Committee.

#### Measurement of intracellular and plasma amino-acid levels

Cells were washed three times with ice-cold phosphate-buffered saline (PBS) and homogenized in 80% methanol containing phenyl-d5-alanine as an internal standard for extraction, and then centrifuged (15 000 r.p.m. for 15 min at 4 °C) to obtain supernatants. Samples were evaporated and then resuspended in a small volume of water before derivatization. For amino-acid analysis in plasma, mouse blood samples were collected by cardiocentesis, mixed with ethylenediaminetetraacetic acid and immediately cooled on ice. Plasma was separated by centrifugation at 800 *g* for 15 min at 4 °C, and was deproteinized in a final concentration of 50% acetonitrile. The supernatant was used for the following analysis.

Amino-acid analysis using high-performance liquid chromatography and electrospray ionization tandem mass spectrometry was carried out as described previously<sup>41</sup> with minor modifications. Samples were mixed with APDSTAG Wako Amino Acids Internal Standard Mixture Solution and derivatized with 3-aminopyridyl-N-hydroxysuccinimidyl carbamate. Derivatized samples were injected onto an Agilent 1200 series liquid chromatography system (Agilent Technologies, Waldbrunn, Germany) coupled to an API 4000 triple quadrupole mass spectrometer (Applied Biosystems-MDS Sciex, Concord, ON, Canada). An Inertsil C8-3 column (GL Sciences Inc., Tokyo, Japan) and the mobile phase A (APDSTAGTM Wako Eluent) and B (water and acetonitrile) were used for separation.

#### Measurement of OCR and ECAR

OCR and ECAR were measured using the Seahorse XF24 Flux Analyzer (Seahorse Bioscience, North Billerica, MA, USA). A total of  $3 \times 10^5$  cells per well were seeded on a gelatin-coated plate in regular medium. The medium was replaced with XF Assay Medium (Seahorse Bioscience) supplemented with 1 mM pyruvate, 10 mM glucose and 2 mM Gln (pH 7.4) 1 h before measurement. Oligomycin, carbonyl cyanide 4-(trifluoromethoxy)phenylhydrazone and antimycin/rotenone were added by the Flux Analyzer when indicated.

#### Detection of mitochondrial membrane potential and cellular ROS

Mitochondrial membrane potential and intracellular ROS production were measured using TMRE (tetramethylrhodamine, ethyl ester) Mitochondrial Membrane Potential Assay Kit (ab113852) and DCFDA Cellular ROS Detection Assay Kit (ab113851), respectively (both from Abcam, Cambridge, UK). For the TMRE assay, cells were incubated with 100 nM of TMRE for 15 min at 37 °C with 5% CO<sub>2</sub> and then suspended in PBS with 0.2% FBS. For the ROS detection assay, cells were harvested and incubated with 10  $\mu$ M of DCFDA (intracellular ROS) for 30 min and MitoSOX (mitochondrial ROS, Thermo Scientific, Waltham, MA, USA) at 37 °C with 5% CO<sub>2</sub>. Fluorescence intensity for both procedures was measured by flow cytometry and a microplate reader.

#### Cell viability assay and apoptosis assay

ALL cells were plated at  $1 \times 10^6$  cells in six-well plates and treated with the appropriate reagents. Viable and dead cells were counted using trypan blue assay by the TC20 Automated Cell Counter (BioRad Laboratories, Richmond, CA, USA). Apoptosis was assessed by flow cytometry using Annexin-V/propidium iodide staining (MEBCTO-Apoptosis Kit, MBL Co., Ltd., Nagoya, Japan). All experiments were performed in triplicate.

#### Cell cycle analysis

Cells were washed in PBS and fixed in 70% cold ethanol overnight at –20 °C. Fixed cells were washed in PBS, incubated in PBS containing RNase (250  $\mu$ g/ml) for 30 min at 37 °C and then stained with propidium iodide (Thermo Scientific). Fluorescence intensities were measured by flow cytometry and cell population analysis was performed using the FlowJo software (Tree-star Inc., Ashland, OR, USA).

#### Generation of L-asp-resistant cells

L-asp-resistant cells were established by sequential incubation of parental cells with increasing concentrations of L-asp from 0.01 to 1.0 U/ml for 6 months in resistant cells from 697 cells (697-R).

#### Measurement of mitochondrial DNA copy number and mitochondrial mass

The relative ratio of mitochondrial DNA to nuclear genomic DNA was measured using the Human Mitochondrial DNA Monitoring Primer Set Ratio kit (Takara Bio, Shiga, Japan). For measurement of mitochondrial mass, cells were incubated with 100 nM of MitoTracker green (Thermo Scientific) for 30 min, and fluorescence intensities were measured by flow cytometry.

#### Immunofluorescence analysis

Cells were fixed in cold methanol for 5 min. After blocking with PBS containing 1% bovine serum albumin and 0.01% Triton X-100 for 1 h at 4 °C, the cells were incubated with anti-LC3B (Sigma-Aldrich Co.) and/or human CD45-FITC antibodies (Becton, Dickinson and Company, Franklin Lakes, NJ, USA) overnight at 4 °C. Bound antibodies were visualized using Alexa Fluor 488 anti-mouse IgG antibody (Invitrogen, Carlsbad, CA, USA). The cells were mounted in VECTASHIELD Mounting Medium with DAPI (Vector Laboratories, Burlingame, CA, USA). Images were obtained by confocal fluorescence microscopy (Nikon, Tokyo, Japan).

#### Electron microscopy

The cells were fixed with 2.5% glutaraldehyde in 0.1 M PBS overnight. They were washed with 0.1 M PBS and post-fixed with 1% O<sub>3</sub>O<sub>4</sub> buffered in 0.1 M PBS for 2 h. Then, the cells were dehydrated in a graded series of ethanol solutions and embedded in Epon 812. Ultrathin (90 nm) sections were collected on copper grids, double-stained with uranyl acetate and lead citrate and examined by transmission electron microscopy (H-7100, Hitachi, Tokyo, Japan).

#### Gene expression array analysis

Gene expression profiling of ALL cells was performed as previously reported.<sup>42</sup> GO analysis was performed using DAVID (<https://david.ncicfcrf.gov/home.jsp>) and gene set enrichment analysis (<http://www.broadinstitute.org/gsea/index.jsp>). The microarray data from this publication have been submitted to the GEO database (<http://www.ncbi.nlm.nih.gov/geo/>) and assigned the identifier GSE94289.

#### Real-time polymerase chain reaction

Quantitative real-time polymerase chain reaction (PCR) was carried out using TaqMan polymerase with SYBR Green fluorescence (KAPA SYBR FAST qPCR Master Mix: NIPPON Genetics, Tokyo, Japan) on an ABI PRISM 7300 Sequence Detector (Applied Biosystems, Concord, ON, Canada). Real-time RT-qPCR analysis was performed using specific primers (Supplementary Table S1).



## Western blotting

Western blotting analysis was performed as previously reported.<sup>42</sup> Antibodies for LC3B (L7543),  $\beta$ -actin (A5441) and asparagine synthetase (A6485) were purchased from Sigma-Aldrich; ATF4 (L0911) was from Santa Cruz Biotechnology (Dallas, TX, USA); p53 (OP43L) was from Calbiochem (San Diego, CA, USA); cleaved PARP (#9541), cleaved CASP3 (#9661), CASP3 (#9662), CHOP (#2895), BECN1 (#4122) and ATG5 (#12994) were from Cell Signaling (Danvers, MA, USA);  $\gamma$ H2AX (ab11174) was from Abcam.

## Transduction of shRNA or siRNA

shRNA oligonucleotides for *TP53* (target sequence: 5'-GACTCCAGTG GTAATCTAC-3') were annealed and inserted into the pGreenPuro vector (System Biosciences, Palo Alto, CA, USA). Lentivirus was prepared using HEK293T cells and the pPACK Packaging Kit (System Biosciences) according to the manufacturer's instructions. Virus titer was measured in IFU/ml by a RT-PCR-based method using the Global UltraRapid Lentiviral Titer Kit (System Biosciences). Cells were infected with 5 multiplicity of infection (PFU/cell) of lentivirus with either an empty vector (as a control) or p53-shRNA vector using TransDux (System Biosciences).

The siRNA for *TP53* (M-003329-03-0005), *BECN1* (M-010552-01-0005), *ATG5* (M-004374-04-0005), *ATG7* (M-020112-01-0005) and non-targeting negative control (D-001206-14-05) were obtained from Thermo Scientific Dharmacon. Cells were transfected with 10 nM of each siRNA using the HVJ Envelope Vector Kit (GENOMEONE-Neo, Ishihara Sangyo), according to the manufacturer's instructions.

## Recombinant Adenovirus infection

The *TP53* adenovirus was prepared and cells were infected as previously described.<sup>43</sup> As a control, an Ad-LacZ adenovirus encoding the  $\beta$ -galactosidase gene was constructed from the cosmid pXCAiLacZ (Takara Bio).

## Mutation analysis in TP53 by direct sequencing

Mutations within coding exons in the *TP53* gene were analyzed by direct DNA sequencing. DNA fragments were amplified by PCR using primer pairs described previously (<http://www-p53.iarc.fr>) and then PCR products were sequenced by primer for each exon.

## Statistics

The experiments performed in ALL cell lines were performed independently in triplicate. All *P*-values were two-tailed and considered significant at  $< 0.05$ . Statistical analyses were performed using the statistical software EZR (Saitama Medical Center, Jichi Medical University, Saitama, Japan).<sup>44</sup> We analyzed drug synergism using the Chou-Talalay median-effect method<sup>45</sup> and used CalcuSyn software (Biosoft, Cambridge, UK) to calculate the combination index and perform isobologram analysis of drug interactions.

## CONFLICT OF INTEREST

The authors declare no conflict of interest.

## ACKNOWLEDGEMENTS

We are deeply grateful to N Hattori (Juntendo University, Japan) for use of the extracellular flux analyzer and H Sato, A Hagiwara and Y Noguchi (Ajinomoto Co., Inc., Japan) for the intracellular amino-acid analysis. We thank U Kevin, S Ikeda and T Muramatsu (Tokyo Medical and Dental University, Japan) for editing this article. We also thank R Mori and K Ayako (Tokyo Medical and Dental University, Japan) for technical assistance in lentivirus preparation and gene expression arrays. This study was supported in part by Grant-in-Aid for Scientific Research (C:15K08301) and Grant-in-Aid for Scientific Research on Innovative Areas "Conquering cancer through NEO-dimensional systems understandings" (15H05908) from JSPS and MEXT, and the Joint Usage/Research Program of MRI, TMDU.

## REFERENCES

- Locatelli F, Schrappe M, Bernardo ME, Rutella S. How I treat relapsed childhood acute lymphoblastic leukemia. *Blood* 2012; **120**: 2807–2816.
- Curran E, Stock W. How I treat acute lymphoblastic leukemia in older adolescents and young adults. *Blood* 2015; **125**: 3702–3710.

- Oettgen HF, Old LJ, Boyse EA, Campbell HA, Philips FS, Clarkson BD *et al*. Inhibition of leukemias in man by L-asparaginase. *Cancer Res* 1967; **27**: 2619–2631.
- Hongo T, Yajima S, Sakurai M, Horikoshi Y, Hanada R. *In vitro* drug sensitivity testing can predict induction failure and early relapse of childhood acute lymphoblastic leukemia. *Blood* 1997; **89**: 2959–2965.
- Kaspers GJ, Veerman AJ, Pieters R, Van Zantwijk CH, Smets LA, Van Wering ER *et al*. In vitro cellular drug resistance and prognosis in newly diagnosed childhood acute lymphoblastic leukemia. *Blood* 1997; **90**: 2723–2729.
- Aslanian AM, Kilberg MS. Multiple adaptive mechanisms affect asparagine synthetase substrate availability in asparaginase-resistant MOLT-4 human leukaemia cells. *Biochem J* 2001; **358**: 59–67.
- Stams WA, den Boer ML, Holleman A, Appel IM, Beverloo HB, van Wering ER *et al*. Asparagine synthetase expression is linked with L-asparaginase resistance in TEL-AML1-negative but not TEL-AML1-positive pediatric acute lymphoblastic leukemia. *Blood* 2005; **105**: 4223–4225.
- Su N, Pan YX, Zhou M, Harvey RC, Hunger SP, Kilberg MS. Correlation between asparaginase sensitivity and asparagine synthetase protein content, but not mRNA, in acute lymphoblastic leukemia cell lines. *Pediatr Blood Cancer* 2008; **50**: 274–279.
- Stams WA, den Boer ML, Beverloo HB, Meijerink JP, Stigter RL, van Wering ER *et al*. Sensitivity to L-asparaginase is not associated with expression levels of asparagine synthetase in t(12;21)+ pediatric ALL. *Blood* 2003; **101**: 2743–2747.
- Holleman A, Cheok MH, den Boer ML, Yang W, Veerman AJ, Kazemier KM *et al*. Gene-expression patterns in drug-resistant acute lymphoblastic leukemia cells and response to treatment. *N Engl J Med* 2004; **351**: 533–542.
- Fine BM, Kaspers GJ, Ho M, Loonen AH, Boxer LM. A genome-wide view of the *in vitro* response to L-asparaginase in acute lymphoblastic leukemia. *Cancer Res* 2005; **65**: 291–299.
- Hermanova I, Zaliova M, Trka J, Starkova J. Low expression of asparagine synthetase in lymphoid blasts precludes its role in sensitivity to L-asparaginase. *Exp Hematol* 2012; **40**: 657–665.
- Choi AM, Ryter SW, Levine B. Autophagy in human health and disease. *N Engl J Med* 2013; **368**: 651–662.
- Amaravadi RK, Lippincott-Schwartz J, Yin XM, Weiss WA, Takebe N, Timmer W *et al*. Principles and current strategies for targeting autophagy for cancer treatment. *Clin Cancer Res* 2011; **17**: 654–666.
- Rebecca VW, Amaravadi RK. Emerging strategies to effectively target autophagy in cancer. *Oncogene* 2016; **35**: 1–11.
- Yu M, Henning R, Walker A, Kim G, Perroy A, Alessandro R *et al*. L-asparaginase inhibits invasive and angiogenic activity and induces autophagy in ovarian cancer. *J Cell Mol Med* 2012; **16**: 2369–2378.
- Hermanova I, Arruabarrena-Aristorena A, Valis K, Nuskova H, Alberich-Jorda M, Fiser K *et al*. Pharmacological inhibition of fatty-acid oxidation synergistically enhances the effect of L-asparaginase in childhood ALL cells. *Leukemia* 2015; **30**: 209–218.
- Song P, Ye L, Fan J, Li Y, Zeng X, Wang Z *et al*. Asparaginase induces apoptosis and cytoprotective autophagy in chronic myeloid leukemia cells. *Oncotarget* 2015; **6**: 3861–3873.
- Sherman BT, Huang da W, Tan Q, Guo Y, Bour S, Liu D *et al*. DAVID Knowledgebase: a gene-centered database integrating heterogeneous gene annotation resources to facilitate high-throughput gene functional analysis. *BMC Bioinformatics* 2007; **8**: 426.
- Subramanian A, Tamayo P, Mootha VK, Mukherjee S, Ebert BL, Gillette MA *et al*. Gene set enrichment analysis: a knowledge-based approach for interpreting genome-wide expression profiles. *Proc Natl Acad Sci USA* 2005; **102**: 15545–15550.
- Klionsky DJ, Abdalla FC, Abeliovich H, Abraham RT, Acevedo-Arozena A, Adeli K *et al*. Guidelines for the use and interpretation of assays for monitoring autophagy. *Autophagy* 2012; **8**: 445–544.
- Ueno T, Ohtawa K, Mitsui K, Kodera Y, Hiroto M, Matsushima A *et al*. Cell cycle arrest and apoptosis of leukemia cells induced by L-asparaginase. *Leukemia* 1997; **11**: 1858–1861.
- Reddy PN, Sargin B, Choudhary C, Stein S, Grez M, Muller-Tidow C *et al*. SOCS1 cooperates with FLT3-ITD in the development of myeloproliferative disease by promoting the escape from external cytokine control. *Blood* 2012; **120**: 1691–1702.
- Velasco-Hernandez T, Hyrenius-Wittsten A, Rehn M, Bryder D, Cammenga J. HIF-1 $\alpha$  can act as a tumor suppressor gene in murine acute myeloid leukemia. *Blood* 2014; **124**: 3597–3607.
- Ye J, Kumanova M, Hart LS, Sloane K, Zhang H, De Panis DN *et al*. The GCN2-ATF4 pathway is critical for tumour cell survival and proliferation in response to nutrient deprivation. *EMBO J* 2010; **29**: 2082–2096.

- 26 Sablina AA, Budanov AV, Ilyinskaya GV, Agapova LS, Kravchenko JE, Chumakov PM. The antioxidant function of the p53 tumor suppressor. *Nat Med* 2005; **11**: 1306–1313.
- 27 Ranjan A, Iwakuma T. Non-canonical cell death induced by p53. *Int J Mol Sci* 2016; **17**: 2068.
- 28 Amaravadi RK, Yu D, Lum JJ, Bui T, Christophorou MA, Evan GI *et al*. Autophagy inhibition enhances therapy-induced apoptosis in a Myc-induced model of lymphoma. *J Clin Invest* 2007; **117**: 326–336.
- 29 Degenhardt K, Mathew R, Beaudoin B, Bray K, Anderson D, Chen G *et al*. Autophagy promotes tumor cell survival and restricts necrosis, inflammation, and tumorigenesis. *Cancer Cell* 2006; **10**: 51–64.
- 30 Maiuri MC, Zalckvar E, Kimchi A, Kroemer G. Self-eating and self-killing: crosstalk between autophagy and apoptosis. *Nat Rev Mol Cell Biol* 2007; **8**: 741–752.
- 31 Lorenzi PL, Claerhout S, Mills GB, Weinstein JN. A curated census of autophagy-modulating proteins and small molecules: candidate targets for cancer therapy. *Autophagy* 2014; **10**: 1316–1326.
- 32 Bonapace L, Bornhauser BC, Schmitz M, Cario G, Ziegler U, Niggli FK *et al*. Induction of autophagy-dependent necroptosis is required for childhood acute lymphoblastic leukemia cells to overcome glucocorticoid resistance. *J Clin Invest* 2010; **120**: 1310–1323.
- 33 Laane E, Tamm KP, Buentke E, Ito K, Kharaziha P, Oscarsson J *et al*. Cell death induced by dexamethasone in lymphoid leukemia is mediated through initiation of autophagy. *Cell Death Differ* 2009; **16**: 1018–1029.
- 34 Polak A, Kiliszek P, Sewastianik T, Szydowski M, Jablonska E, Bialopiotrowicz E *et al*. MEK inhibition sensitizes precursor B-cell acute lymphoblastic leukemia (B-ALL) cells to dexamethasone through modulation of mTOR activity and stimulation of autophagy. *PLoS One* 2016; **11**: e0155893.
- 35 Bush A, Cunningham S, de Blic J, Barbato A, Clement A, Epaud R *et al*. European protocols for the diagnosis and initial treatment of interstitial lung disease in children. *Thorax* 2015; **70**: 1078–1084.
- 36 Barrera V, Hiscott PS, Craig AG, White VA, Milner DA, Beare NA *et al*. Severity of retinopathy parallels the degree of parasite sequestration in the eyes and brains of malawian children with fatal cerebral malaria. *J Infect Dis* 2015; **211**: 1977–1986.
- 37 Eng CH, Wang Z, Tkach D, Toral-Barza L, Ugwonalu S, Liu S *et al*. Macroautophagy is dispensable for growth of KRAS mutant tumors and chloroquine efficacy. *Proc Natl Acad Sci USA* 2016; **113**: 182–187.
- 38 Rosenfeldt MT, O'Prey J, Morton JP, Nixon C, MacKay G, Mrowinska A *et al*. p53 status determines the role of autophagy in pancreatic tumour development. *Nature* 2013; **504**: 296–300.
- 39 Lee SW, Kim HK, Lee NH, Yi HY, Kim HS, Hong SH *et al*. The synergistic effect of combination temozolomide and chloroquine treatment is dependent on autophagy formation and p53 status in glioma cells. *Cancer Lett* 2015; **360**: 195–204.
- 40 Stengel A, Schnittger S, Weissmann S, Kuznia S, Kern W, Kohlmann A *et al*. TP53 mutations occur in 15.7% of ALL and are associated with MYC-rearrangement, low hypodiploidy, and a poor prognosis. *Blood* 2014; **124**: 251–258.
- 41 Shimbo K, Oonuki T, Yahashi A, Hirayama K, Miyano H. Precolumn derivatization reagents for high-speed analysis of amines and amino acids in biological fluid using liquid chromatography/electrospray ionization tandem mass spectrometry. *Rapid Commun Mass Spectrom* 2009; **23**: 1483–1492.
- 42 Fujiwara N, Inoue J, Kawano T, Tanimoto K, Kozaki K, Inazawa J. miR-634 activates the mitochondrial apoptosis pathway and enhances chemotherapy-induced cytotoxicity. *Cancer Res* 2015; **75**: 3890–3901.
- 43 Inoue J, Misawa A, Tanaka Y, Ichinose S, Sugino Y, Hosoi H *et al*. Lysosomal-associated protein multispanspanning transmembrane 5 gene (LAPTM5) is associated with spontaneous regression of neuroblastomas. *PLoS One* 2009; **4**: e7099.
- 44 Kanda Y. Investigation of the freely available easy-to-use software 'EZ' for medical statistics. *Bone Marrow Transplant* 2013; **48**: 452–458.
- 45 Chou TC. Drug combination studies and their synergy quantification using the Chou-Talalay method. *Cancer Res* 2010; **70**: 440–446.



This work is licensed under a Creative Commons Attribution-NonCommercial-ShareAlike 4.0 International License. The images or other third party material in this article are included in the article's Creative Commons license, unless indicated otherwise in the credit line; if the material is not included under the Creative Commons license, users will need to obtain permission from the license holder to reproduce the material. To view a copy of this license, visit <http://creativecommons.org/licenses/by-nc-sa/4.0/>

© The Author(s) 2017

Supplementary Information accompanies this paper on the Oncogene website (<http://www.nature.com/onc>)